POTENTIAL CONTRIBUTIONS OF THE DESDYNI MISSION TO IONOSPHERIC RESEARCH

Franz J Meyer[1], Junsu Kim[2], Ramon Brcic[3], Xiaoqing Pi[4]

[1]Geophysical Institute, University of Alaska Fairbanks, AK, 99775, USA;
email: fmeyer@gi.alaska.edu
[2]Microwaves and Radar Institute, German Aerospace Center (DLR), 82234 Wessling, Germany;
email: Junsu.Kim@dlr.de
[3]Remote Sensing Technology Institute, German Aerospace Center (DLR), 82234 Wessling, Germany;
email: Ramon.Brcic@dlr.de
[4] Jet Propulsion Laboratory, California Institute of Technology, Pasadena, CA 91109, USA;
email: Xiaoqing.Pi@jpl.nasa.gov

1. INTRODUCTION

Ionospheric propagation effects can have significant impact on the signal properties of low-frequency Synthetic Aperture Radar (SAR) systems. Recently, theoretical analyses of ionospheric distortions in low-frequency SAR signals have indicated a multitude of effects that are likely to affect the quality of SAR, interferometric SAR (InSAR), and polarimetric SAR (PolSAR) data [1-6]. Methods have been developed that are able to detect ionospheric effects in SAR data on a wide range of spatial scales and allow high resolution ionospheric mapping with high accuracy [3], [4], [7].

NASA's Deformation, Ecosystem Structure and Dynamics of Ice (DESDynI) mission carries a spaceborne L-band synthetic aperture radar (SAR) with multiple polarizations to provide information on solid earth deformation, terrestrial vegetation structure, and ice dynamics. Besides providing improved performance and reliability of SAR for monitoring surface deformation, the L-band carrier frequency provides a means for mapping properties of the ionosphere with high spatial resolution and unprecedented spatial coverage.

This paper describes the performance and benefits of DESDynI for ionospheric mapping. Specifically, we quantify the type, sensitivity, and accuracy of ionospheric measurements derived by a DESDynI-like system. We also analyze the achievable spatial and temporal sampling of ionospheric constituents at different areas on the globe and assess the value of the derived information for specific ionospheric research topics.

After summarizing the physical origin of ionospheric signals in SAR data, Section 2 introduces several methods for extracting ionospheric information from DESDynI data. For each method, information on the measurement principle is provided and the range of extractable ionospheric parameters is determined. A first concept for an optimized ionospheric processor is shown that extends the performance of existing technology by maximizing the exploited information and increasing estimation robustness. An error analysis of the presented technology is shown in Section 3, where achievable accuracies of ionospheric measurements are analyzed for different retrieval methods. In Section 4 the benefit of SAR-based ionospheric data for ionospheric research is evaluated. In examples we examine its value for analyzing turbulent ionospheric processes in polar and equatorial regions, and for evaluating the structure of traveling ionospheric disturbances (TIDs) at various spatial scales.

2. MAPPING IONOSPHERIC TEC FROM DESDYNI DATA

2.1. Background

The one-way phase delay experienced by a SAR signal is given by

$$\phi(f) = -2\pi f \frac{1}{10^6} \int \frac{N_{iono}(f,h)}{c} dh \approx 2\pi \frac{K}{cf_0} TEC \tag{1}$$

where $TEC = \int N_{iono}(f,h) dh$ is the ionospheric *total electron content* integrated along the vertical, f_0 is the signal frequency, N_{iono} is the ionospheric refractivity, and $K = 1/2 \cdot e/(4\pi^2 m \varepsilon_0) = 40.28[m^3/s^2]$. In addition to the phase delay in Eq. (1), the ionosphere also introduces a rotation of the polarization orientation of a traversing microwave signal. The magnitude of this effect, known as *Faraday rotation (FR)*, for a one-way vertical propagation through the ionosphere is given by

$$\Omega = \phi(f_0) \cdot \frac{f_H}{f_0} \cos(\theta) = \frac{K}{f_0^2} B \cos(\theta) TEC \tag{2}$$

All ionospheric effects on SAR imaging, SAR interferometry, and SAR polarimetry can be derived by evaluating Eqs. (1) and (2). While Equation (2) can be used to investigate effects on the signal's polarimetric signature, an analysis of the first terms of a Taylor series expansion of Equation (1)

$$\phi(f) = -\frac{4\pi}{c_0} \frac{40.28}{f_0} TEC + \frac{4\pi}{c_0} \frac{40.28}{f_0^2} TEC \cdot (f - f_0) - \frac{4\pi}{c_0} \frac{40.28}{f_0^3} TEC \cdot (f - f_0)^2 \tag{3}$$

allows a quantitative evaluation of ionospheric effects on SAR signal phase, signal envelope, and SAR signal chirp rate (first to third component in Eq. (3), respectively). Eqs. (1)-(3) can serve as basis of ionospheric mapping methods using model-based inversion techniques.

2.2. Applicable Mapping Methods

A variety of methods for ionospheric correction in SAR, InSAR, and PolSAR data have been published in recent years by several authors. These methods can be grouped into *i)* range spectrum-based ([8];[2];[9]), and *ii)* azimuth spectrum-based techniques ([10];[9]), reflecting the SAR signal component that is used by the algorithms. Variations of these methods have been developed for application to single images, PolSAR ([11];[4]), and InSAR data. In the paper, the principle and sensitivities of the various methods will be shortly summarized.

2.3. Advanced Ionospheric Mapping Using Integrated Detection Concepts

The properties of ionospheric effects in SAR images and the performance of ionospheric correction methods are both constrained by various components of the SAR data acquisition process. The most relevant of these components are the SAR system design and operational mode, the properties of the imaged scene, the ionospheric conditions, and the geographic location. An improved detection and correction algorithm must consider all these constraints, as well as adjust detection strategies according to changes in the data acquisition conditions.

An improved hybrid mapping concept will be presented that exploits synergies between existing correction principles. The approach formulates the ionospheric mapping problem as an inverse problem that is finding an optimized solution for $TEC(x,y)$ by combining a set of initial detector estimates in either a least-squares adjustment formulated as a Gauss-Markov model or a Kalman-filtering procedure.

3. ACCURACY ESTIMATIONS

Performance estimations will be presented for a wide range of ionospheric mapping methods as a function of system parameters, geographic location, and processing strategy. Some examples of accuracy estimates are shown in Figure 1 where the achievable accuracy of Faraday rotation and split-spectrum-based processing methods are presented. These results are compared to the structure and magnitude of ionospheric signals to provide a basis for an analysis of SAR benefits to ionospheric research.

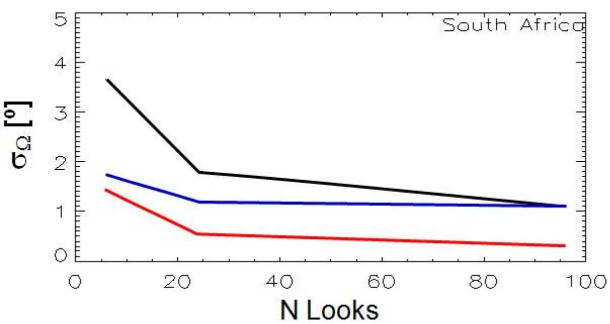

a)

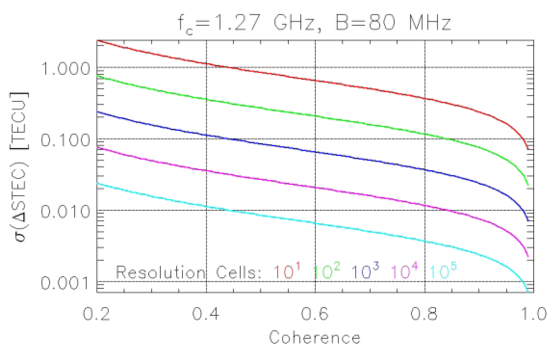

b)

Figure 1: Examples of accuracy estimates for ionospheric mapping: a) accuracy of three different Faraday rotation measurements as a function of number of looks; b) estimation accuracy of TEC measurements from split-bandwidth processing as a function of number of looks and InSAR coherence. Results are based on DESDynI-like system parameters.

4. POTENTIAL APPLICATIONS TO IONOSPHERIC RESEARCH

We will analyze the usefulness of SAR-derived ionospheric information for the analysis of turbulent ionospheric structures in polar and equatorial regions. The analysis considers measurement sensitivities and absolute accuracies, as well as temporal and spatial resolution. It will also examine how the temporal sampling of ionospheric phenomena can be increased if DESDynI observations are combined with other current and future low-frequency SAR sensors. As an example of the potential spatial coverage and measurement sensitivity provided by SAR, Figure 2 shows TEC estimates derived along a swath of full-polarimetric ALOS PALSAR data acquired over Alaska. Here, TEC was estimated using Faraday rotation-based techniques. Such ionospheric imaging capability will provide us an opportunity to study ionospheric structures at relatively high spatial resolutions on global scales under various space weather conditions. Studies of polar ionospheric disturbances, dynamics of the middle-latitude ionospheric trough, TID's, and plasma bubbles can particularly benefit from spaceborne ionospheric imaging [6]. For Earth science research, observations of ionospheric responses to the solid Earth, atmospheric and oceanic activities can also benefit from SAR-based ionospheric imaging.

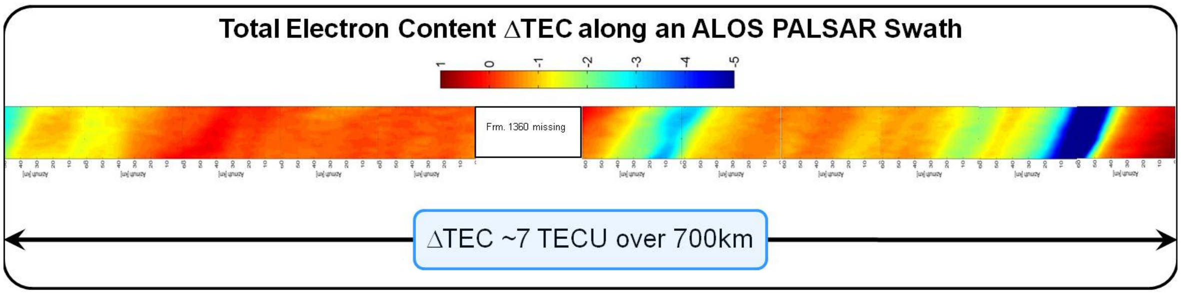

Figure 2: Example of TEC variation along along a swath of full-pol ALOS PALSAR data. TEC estimates have been derived using Faraday rotation-based mapping techniques.

5. CONCLUSIONS

Our findings show that L-band SAR data provided by DESDynI is valuable for studying ionospheric activity on a wide range of spatial and temporal scales. The analysis demonstrates that phase advance, group delay, and Faraday rotation can be measured with sufficient accuracy and spatial resolution to produce spatial maps of small-scale ionospheric features. While one SAR system cannot provide instantaneous global ionospheric data, a combination of all current and future low-frequency SAR sensors can produce ionospheric information of sufficient temporal resolution that is of significant relevance to the ionospheric science community.

11. REFERENCES

[1] Z.-W. Xu, J. Wu, and Z.-S. Wu, "A Survey of Ionospheric Effects on Space-based Radar," Waves in Random Media, vol. 14, pp. 189–273, 2004.

[2] F. Meyer, R. Bamler, N. Jakowski, and T. Fritz, "The Potential of Low-Frequency SAR Systems for Mapping Ionospheric TEC Distributions," Geoscience and Remote Sensing Letters, vol. 2, no. 4, pp. 560–564, 2006.

[3] F. Meyer and J. Nicoll, "Prediction, Detection, and Correction of Faraday Rotation in Full-Polarimetric L-Band SAR Data," IEEE Trans. Geosci. Remote Sens., vol. 46, no. 10, pp. 3076-3086, 2008.

[4] A. Freeman, and S. Saatchi, "On the Detection of Faraday Rotation in Linearly Polarized L-Band SAR Backscatter Signatures," Trans. On Geoscience and Remote Sensing, vol. 42, No. 8, pp. 1607–1616, 2004.

[5] A. Gray, K. Mattar, and G. Sofko, "Influence of ionospheric electron density fluctuations on satellite radar interferometry," Geophys. Res. Lett., vol. 27, no. 10, pp. 1451–1454, May 2000.

[6] Pi, X., A. Freeman, B. Chapman, P. Rosen, Z. Li, "Imaging ionospheric inhomogeneities using spaceborne synthetic aperture radar," *J. Geophys. Res*., in press, 2011.

[7] J. Nicoll and F. Meyer, "Mapping the Ionosphere Using L-Band SAR Data**,"** Proceedings of IGARSS'08 Conference, 2008, Boston, vol. 2, pp. 537–540, 2008.

[8] Rosen, P.A., Hensley, S., Zebker, H.A.; Webb, F. H., Fielding, E. J., "Surface deformation and coherence measurements of Kilauea Volcano, Hawaii, from SIR C radar interferometry," *Journal of Geophysical Research*, vol. 101 (E10):23,10923,126, doi:10.1029/96JE01459.

[9] Schneider, R.Z. and K. Papathanassiou, "Ionospheric Correction by Means of Coherent Scatterers," *Proceedings of EUSAR'08*, vol. 3, 105–108, 2008.

[10] Meyer, F., and J. Nicoll, "The Impact of the Ionosphere on Interferometric SAR Processing**,"** Proceedings of IGARSS'08 Conference, 2008, Boston, vol. 2, pp. 391–394.

[11] Bickel, S.H. and R.H.T. Bates. Effects of magneto-ionic propagation on the polarization scattering matrix, *Proc. IRE*, *53*, 1089-1091. 1965.